Initial partonic eccentricity fluctuations in a multiphase transport model

L. Ma,[1,2] G. L. Ma,[1,*] and Y. G. Ma[1,3,†]
[1]*Shanghai Institute of Applied Physics, Chinese Academy of Sciences, Shanghai 201800, China*
[2]*University of Chinese Academy of Sciences, Beijing 100049, China*
[3]*ShanghaiTech University, Shanghai 200031, China*
(Received 28 June 2016; revised manuscript received 1 October 2016; published 27 October 2016)

Initial partonic eccentricities in Au + Au collisions at center-of-mass energy $\sqrt{s_{NN}} = 200$ GeV are investigated by using a multiphase transport model with a string-melting scenario. The initial eccentricities in different order of harmonics are studied by using participant and cumulant definitions. Eccentricity in terms of second-, fourth- and sixth-order cumulants as a function of number of participant nucleons are compared systematically with the traditional participant definition. The ratio of the cumulant eccentricities $\varepsilon\{4\}/\varepsilon\{2\}$ and $\varepsilon\{6\}/\varepsilon\{4\}$ are studied in comparison with the ratio of the corresponding flow harmonics. The conversion coefficients (v_n/ε_n) are explored up to fourth-order harmonics based on the cumulant method. Furthermore, studies on transverse momentum (p_T) and pseudorapidity (η) dependencies of eccentricities and their fluctuations are presented. As in ideal hydrodynamics, initial eccentricities are expected to be closely related to the final flow harmonics in relativistic heavy-ion collisions, studies of the fluctuating initial condition in the AMPT model will shed light on the tomography properties of the initial source geometry.

DOI: 10.1103/PhysRevC.94.044915

I. INTRODUCTION

In ultrahigh-energy heavy-ion collisions, the pressure gradient in the overlap zone is large enough to translate the initial coordinate space anisotropy into the final-state momentum space anisotropy, which can be experimentally observed as anisotropic flow. Anisotropic flow as a typical collective behavior of emitted particles has been proved to be a good observable to study the new matter in relativistic heavy-ion collisions providing information on equation-of-state and the transport properties of the matter created [1,2]. One of the most striking experimental results ever obtained in relativistic heavy-ion collisions is the strong elliptic flow (v_2). The fluid-like behavior of matter created in the early stage leads to the conclusion that the quark gluon plasma is like a nearly perfect liquid [3–8]. Due to the fluid-like properties of elliptic flow v_2, hydrodynamic models have been widely used to make predictions, and it was suggested that the final-state anisotropy inherits information from the initial state and carries additional information on the system evolution [9–11]. Thus, measurements of the elliptic flow coefficient v_2 provides essential information about the hot and dense matter created in relativistic heavy-ion collisions.

Besides the elliptic flow v_2 measurement, higher-order harmonic flow coefficients defined as v_n $(n = 3,4,5)$ have drawn much more attention in both experiment and model studies in recent years as higher harmonics are suggested to be sensitive to the initial partonic dynamics [12–17]. The importance of fluctuations was first realized in the simulations with a multiphase transport (AMPT) model, showing that the fluctuating initial source geometry transfers to the final momentum space during the system expansion leading to nonzero higher odd-order harmonic flow coefficients [18]. It was also realized that higher harmonics such as triangular flow v_3 is particularly sensitive not only to the initial condition but also to the shear viscosity η which reflects the properties of the source in the early stage [19,20]. Studies also suggest that the elliptic flow and higher harmonic flow fluctuations on the event-by-event basis elucidate both the system dynamics and new phenomena occurring in the very beginning of collisions [21–23]. Experimental measurements on an event-by-event basis were done for the elliptic flow v_2 fluctuation study in Au + Au collisions at $\sqrt{s_{NN}} = 200$ GeV in the PHOBOS and STAR experiments [24–27]. It suggests that the close correlation between anisotropic flow fluctuation and the fluctuations of the initial source geometry carry important information of the viscosity and other properties of the matter created in heavy-ion collisions [28,29].

Significant attention has been paid to the studies of the effect of initial geometry fluctuations on the final flow observables [30–34]. The essential role of the collision geometry was realized when one looks into the flow harmonics of different collision systems scaled by initial eccentricities [35]. The phenomena observed strongly suggest that the partonic participant eccentricity is responsible for the development of the final anisotropic flow. Higher-order eccentricities are also suggested to be closely related to the final higher-order harmonic flow. The triangular flow v_3 and higher harmonics are suggested to arise from event-by-event initial fluctuations, which lead to finite value even in most-central collisions. Thus, the study of initial eccentricity and fluctuation is crucial for understanding the final flow and flow fluctuations [36,37]. Therefore, the study of the event-by-event flow response to the initial eccentricity in model simulation is important for a quantitative study of the source evolution properties in relativistic heavy-ion collisions.

In this paper, we present specific discussion on source eccentricity and their fluctuation properties in the initial

*glma@sinap.ac.cn
†ygma@sinap.ac.cn

partonic stage of the high-energy heavy-ion collisions using a multiphase transport (AMPT) model. Systematic comparisons are made between cumulant eccentricities and participant eccentricities. Centrality, pseudorapidity, and transverse momentum dependencies of higher-order harmonics are studied in model simulations providing tomographic pictures of the source profile. The results are expected to give additional constraints on the initial source condition. This paper is organized as follows: In Sec. II, a multiphase transport (AMPT) model is briefly introduced. In Sec. III, results and discussions are presented. The last section is a brief summary.

II. BRIEF DESCRIPTION OF MULTIPHASE TRANSPORT MODEL

The multiphase transport model (AMPT) [38] is a useful model for investigating reaction dynamics in relativistic heavy-ion collisions. There are two versions with different scenarios: the default version and the string-melting version, both of which consist of four main components: the initial condition, partonic interactions, hadronization, and hadronic interactions.

In the initial stage, the phase-space distributions of minijet partons and soft string excitations are included, which come from the heavy-ion jet interaction generator (HIJING) [39]. Multiple scatterings lead to fluctuations in local parton-number density and hot spots from both soft and hard interactions which are proportional to local transverse density of participant nucleons. In the AMPT string-melting version, both excited strings and minijet partons are decomposed into partons. Scatterings among partons are then treated according to a parton cascade model—Zhang's parton cascade (ZPC) model, which includes parton-parton elastic scattering with cross sections obtained from the theory calculations [40]. After partons stop interacting with each other, a simple quark coalescence model is used to combine partons into hadrons. Partonic matter is then turned into hadronic matter and the subsequential hadronic interactions are modelled by using a relativistic transport model (ART), including both elastic and inelastic scattering descriptions for baryon-baryon, baryon-meson, and meson-meson interactions [41].

In the ZPC parton cascade model, the differential scattering cross section for partons is defined as

$$\frac{d\sigma_p}{dt} = \frac{9\pi\alpha_s^2}{2}\left(1+\frac{\mu^2}{s}\right)\frac{1}{(t-\mu^2)^2}, \tag{1}$$

where $\alpha_s = 0.47$ is the strong coupling constant, s and t are the usual Mandelstam variables, and μ is the screening mass in partonic matter. Studies show that a multiphase transport model with a string-melting scenario gives a better description of experimental measurements of anisotropic flow harmonics. With a proper choice of parton scattering cross section, data on harmonic flow of charged hadrons measured from experiments for Au + Au collisions at 200GeV can be approximately reproduced [16]. Recent studies also showed that, by changing input parameters, AMPT could quantitatively describe the centrality dependence of elliptic flow and triangular flow in Au + Au [42] as well as the vector mesons in $p+p$ and d + Au systems [43,44].

TABLE I. Centrality classes of AMPT events in Au + Au collisions at $\sqrt{s_{NN}} = 200$ GeV.

Centrality	Impact Parameter range (fm)	$\langle N$ part$\rangle$
0%–10%	0.00–4.42	345.8 ± 0.1
10%–20%	4.42–6.25	263.5 ± 0.1
20%–30%	6.25–7.65	198.2 ± 0.0
30%–40%	7.65–8.83	146.8 ± 0.1
40%-50%	8.83–9.88	106.1 ± 0.0
50%–60%	9.88–10.82	73.8 ± 0.1
60%–70%	10.82–11.68	48.8 ± 0.2

In this work, we use the AMPT string-melting version to simulate Au + Au collisions. Our default sample of simulated events for Au + Au collisions at the center-of-mass energy of 200 GeV is generated with a parton cross section of 3 mb. But we will compare 3 mb with 10 mb when we study the effect of the parton cross section. We make a description of Au + Au collisions at 200GeV with AMPT by using the parameter set $a = 2.2$, $b = 0.5$ (GeV^{-2}) in the Lund string fragmentation function, as shown in Ref. [45]. Particularly, the hadronic-scattering effect and resonance decay effect on the harmonic flow evolution are both taken into account in the model simulation.

Table I shows different centrality classes divided for the simulation samples. The mean number of participant nucleons and corresponding impact parameter for each centrality bin are also shown in the table. In this paper, centrality dependence of all kinds of observables can be measured as a function of mean number of participant nucleons.

III. RESULTS AND DISCUSSION

A. Initial eccentricity and eccentricity fluctuation in partonic stage of multiphase transport model

Experimental measurements of flow coefficients v_n could be affected by event-by-event fluctuations in the initial geometry. Considering the event-by-event fluctuation effect, harmonic flow v_n was proposed to calculate with respect to the participant plane angle $\psi_n\{\text{part}\}$ under the participant coordinate system instead of the traditional reaction plane angle ψ_{RP} in the model simulation [46]. The above method for the calculation of v_n is referred to as the participant plane method which has been widely used for flow calculations in different models [31]. The participant plane is defined as

$$\psi_n\{\text{part}\} = \frac{1}{n}\left[\arctan\frac{\langle r^n \sin(n\varphi)\rangle}{\langle r^n \cos(n\varphi)\rangle} + \pi\right], \tag{2}$$

where n denotes the nth-order participant plane, r and φ are the position and azimuthal angle of each parton in the AMPT initial stage and the average $\langle\cdots\rangle$ denotes density weighted average. Harmonic flow coefficients with respect to the participant plane are defined as

$$v_n\{\text{part}\} = \langle\cos[n(\phi - \psi_n\{\text{part}\})]\rangle, \tag{3}$$

where ϕ is azimuthal angle of final particle, and the average $\langle\cdots\rangle$ denotes particle average.

Similar to the harmonic flow coefficient, different definitions of the initial anisotropy coefficients are described in Ref. [47]. The one referred to as "participant eccentricity" which characterizes the initial state through the event-by-event distribution of the participant nucleons or partons has been found to be crucial for understanding the initial properties [35]. The participant eccentricity for initial elliptic anisotropy is given by

$$\varepsilon_2\{\text{part}\} = \frac{\sqrt{\left(\sigma_y^2 - \sigma_x^2\right)^2 + 4(\sigma_{xy})^2}}{\sigma_y^2 + \sigma_x^2}, \tag{4}$$

where σ_x, σ_y, σ_{xy} are the event-by-event variances of the participant nucleon or parton distributions along the transverse directions x and y. When transforming the coordinate system to the center-of-mass frame of the participating nucleons, a generalized definition of $\varepsilon_n\{\text{part}\}$ nth-order participant eccentricities takes the form [48]

$$\varepsilon_n\{\text{part}\} = \frac{\sqrt{\langle r^n \cos(n\varphi)\rangle^2 + \langle r^n \sin(n\varphi)\rangle^2}}{\langle r^n\rangle}, \tag{5}$$

where r and φ have the same definitions as for participant plane. Such a definition does not make reference to the direction of the impact parameter vector and instead characterizes the eccentricity through the distribution of participant nucleons or partons which naturally contain the event-by-event fluctuation effect. We simply take this as the participant definition or participant method.

As indicated by Refs. [49,50], under the assumption that v_2 from the participant plane method $v_2\{\text{part}\}$ is proportional to $\varepsilon_2\{\text{part}\}$, the scaling properties are expected to hold for even-higher harmonics. Similar to flow harmonics, it is proposed that initial eccentricity can be quantified by cumulants of $\varepsilon_n\{\text{part}\}$ [47]. The definitions of the second-, fourth-, and sixth-order cumulant of $\varepsilon_n\{\text{part}\}$ are in the form

$$\begin{aligned}
c_{\varepsilon_n\{\text{part}\}}\{2\} &= \left\langle \varepsilon_n^2\{\text{part}\}\right\rangle,\\
c_{\varepsilon_n\{\text{part}\}}\{4\} &= \left\langle \varepsilon_n^4\{\text{part}\}\right\rangle - 2\left\langle \varepsilon_n^2\{\text{part}\}\right\rangle^2,\\
c_{\varepsilon_n\{\text{part}\}}\{6\} &= \left\langle \varepsilon_n^6\{\text{part}\}\right\rangle - 9\left\langle \varepsilon_n^2\{\text{part}\}\right\rangle\left\langle \varepsilon_n^4\{\text{part}\}\right\rangle\\
&\quad + 12\left\langle \varepsilon_n^2\{\text{part}\}\right\rangle^3.
\end{aligned} \tag{6}$$

For the definitions (6), the cumulant definitions here follow the regular way of cumulant flow definitions for two-, four-, and six-particle azimuthal correlations as in Ref. [30]. The corresponding eccentricities defined by cumulants are written as

$$\begin{aligned}
\varepsilon_n^{\text{RC}}\{2\} &= \sqrt{c_{\varepsilon_n\{\text{part}\}}\{2\}},\\
\varepsilon_n^{\text{RC}}\{4\} &= \left(-c_{\varepsilon_n\{\text{part}\}}\{4\}\right)^{1/4},\\
\varepsilon_n^{\text{RC}}\{6\} &= \left(c_{\varepsilon_n\{\text{part}\}}\{6\}/4\right)^{1/6}.
\end{aligned} \tag{7}$$

Here, we use superscript "RC" to denote the definition of the regular cumulant commonly used in many studies [27,31]. Experimentally, as the initial state in heavy-ion collisions is not accessible, the participant plane method is not applicable. Instead, the particle correlation method was proposed for flow study via measurement of correlation of final particles without assuming a certain participant plane. In recent years, a multiparticle cumulants method called the Q-cumulant or direct cumulant method was proposed and widely used in both model and experimental studies [23,31,51–53]. This method uses the Q vector to calculate directly the multiparticle cumulants. The Q vector is defined as

$$Q_n = \sum_{i=1}^{M} e^{in\phi_i}, \tag{8}$$

where ϕ_i is the azimuthal angle in the momentum space of the final particles. The derivation of the expressions for higher-order cumulants is straightforward and the two-, four- and six-particle cumulants can be written as

$$\begin{aligned}
\langle 2\rangle &= \langle e^{in(\phi_1-\phi_2)}\rangle = \frac{|Q_n|^2 - M}{M(M-1)},\\
\langle 4\rangle &= \langle e^{in(\phi_1+\phi_2-\phi_3-\phi_4)}\rangle\\
&= \{|Q_n|^4 + |Q_{2n}|^2 - 2\text{Re}[Q_{2n}Q_n^*Q_n^*]\\
&\quad - 2[2(M-2)|Q_n|^2\\
&\quad - M(M-3)]\}/[M(M-1)(M-2)(M-3)],\\
\langle 6\rangle &= \langle e^{in(\phi_1+\phi_2+\phi_3-\phi_4-\phi_5-\phi_6)}\rangle\\
&= [|Q_n|^6 + 9|Q_{2n}|^2|Q_n|^2 - 6\text{Re}(Q_{2n}Q_nQ_n^*Q_n^*Q_n^*)\\
&\quad + 4\text{Re}(Q_{3n}Q_n^*Q_n^*Q_n^*) - 12\text{Re}(Q_{3n}Q_{2n}^*Q_n^*)\\
&\quad + 18(M-4)\text{Re}(Q_{2n}Q_n^*Q_n^*)\\
&\quad + 4|Q_{3n}|^2 - 9(M-4)(|Q_n|^4 + |Q_{2n}|^2)\\
&\quad + 18(M-2)(M-5)|Q_n|^2 - 6M(M-4)(M-5)]\\
&\quad /[M(M-1)(M-2)(M-3)(M-4)(M-5)].
\end{aligned} \tag{9}$$

Then, the second- and fourth-order cumulants on event average can be given by

$$\begin{aligned}
c_n\{2\} &= \langle\langle 2\rangle\rangle,\\
c_n\{4\} &= \langle\langle 4\rangle\rangle - 2\langle\langle 2\rangle\rangle^2,\\
c_n\{6\} &= \langle\langle 6\rangle\rangle - 9\langle\langle 2\rangle\rangle\langle\langle 4\rangle\rangle + 12\langle\langle 2\rangle\rangle^3,
\end{aligned} \tag{10}$$

where the double brackets denote the weighted average of multiparticle correlations. The weights are the total number of combinations from two-, four-, or six-particle correlations, respectively. For flow coefficient with two-particle cumulants, in order to suppress nonflow from short-range correlations, we divide the whole event into two subevents A and B separated by a pseudorapidity gap of 0.3. Then, $\langle 2\rangle$ in Eq. (9) is modified to be

$$\langle 2\rangle_{\Delta\eta} = \frac{Q_n^A \cdot Q_n^B}{M^A \cdot M^B}, \tag{11}$$

where Q^A and Q^B are the flow vectors from subevents A and B, with M^A and M^B being the corresponding multiplicities.

Then, the harmonic flow v_n can be estimated via cumulants ($n = 2,3,4,\ldots$):

$$v_n\{2\} = \sqrt{c_n\{2\}},$$
$$v_n\{4\} = \sqrt{[4]-c_n\{4\}},$$
$$v_n\{6\} = \sqrt{[6]c_n\{6\}/4}. \quad (12)$$

Estimations of differential flow (for second- and fourth-order cumulants) can be expressed as

$$v_n'\{2\} = \frac{d_n\{2\}}{\sqrt{c_n\{2\}}}, \quad v_n'\{4\} = \frac{d_n\{4\}}{-c_n\{4\}^{3/4}}, \quad (13)$$

where the $d_n\{2\}$ and $d_n\{4\}$ are the two- and four-particle differential cumulants as defined in Ref. [51].

The cumulant method has been applied very successfully in the studies of harmonic flow coefficients and initial eccentricity in heavy-ion collisions [30,54]. It can be extended to the study of initial-state eccentricity fluctuation which can be in a similar way as flow fluctuation study with the cumulant method. The relative fluctuation of ε_n in the cumulant definition can be written as

$$R_{\varepsilon_n} = \sqrt{\frac{\varepsilon_n^2\{2\} - \varepsilon_n^2\{4\}}{\varepsilon_n^2\{2\} + \varepsilon_n^2\{4\}}}. \quad (14)$$

It has been argued that the magnitudes and trends of the eccentricities ε_n imply specifically testable predictions for the magnitude and centrality dependence of flow harmonics v_n [55]. We make a comparison of eccentricities in both cumulant and participant definitions as a function of mean number of participant nucleons $N_{\rm part}$. The upper panels of Fig. 1 show the $N_{\rm part}$ dependence of two-, four- and six-particle cumulant eccentricity $\varepsilon_n\{2\}$, $\varepsilon_n\{4\}$, $\varepsilon_n\{6\}$ and also the participant eccentricity $\varepsilon_n\{\rm part\}$ for different harmonics in Au + Au collisions at 200 GeV in the AMPT model. Cumulant eccentricities are defined with a regular method ($\varepsilon^{\rm RC}$) from multiparticle correlations of the initial partons in the AMPT initial stage. It is found that $\varepsilon_n\{\rm part\}$ ($n = 2,3,4$) are quantitatively smaller than $\varepsilon_n\{2\}$ and larger than $\varepsilon_n\{k\}$ ($k = 4,6$) over the whole centrality range. ε_n from different definitions show a similar trend as a function of mean number of participant nucleons.

In the lower panels of Fig. 1, we plot the relative fluctuations of initial partonic eccentricities in different orders of harmonics as a function of $N_{\rm part}$. In comparison, fluctuation of elliptic eccentricity from the regular cumulant definition exhibits clear dependence on the centrality while higher-order eccentricity fluctuations show little centrality dependence. Fluctuations of eccentricities $R_{\varepsilon_n^{\rm RC}}$ ($n = 2,3,4$) are systematically larger for central collisions than noncentral collisions. For higher-order

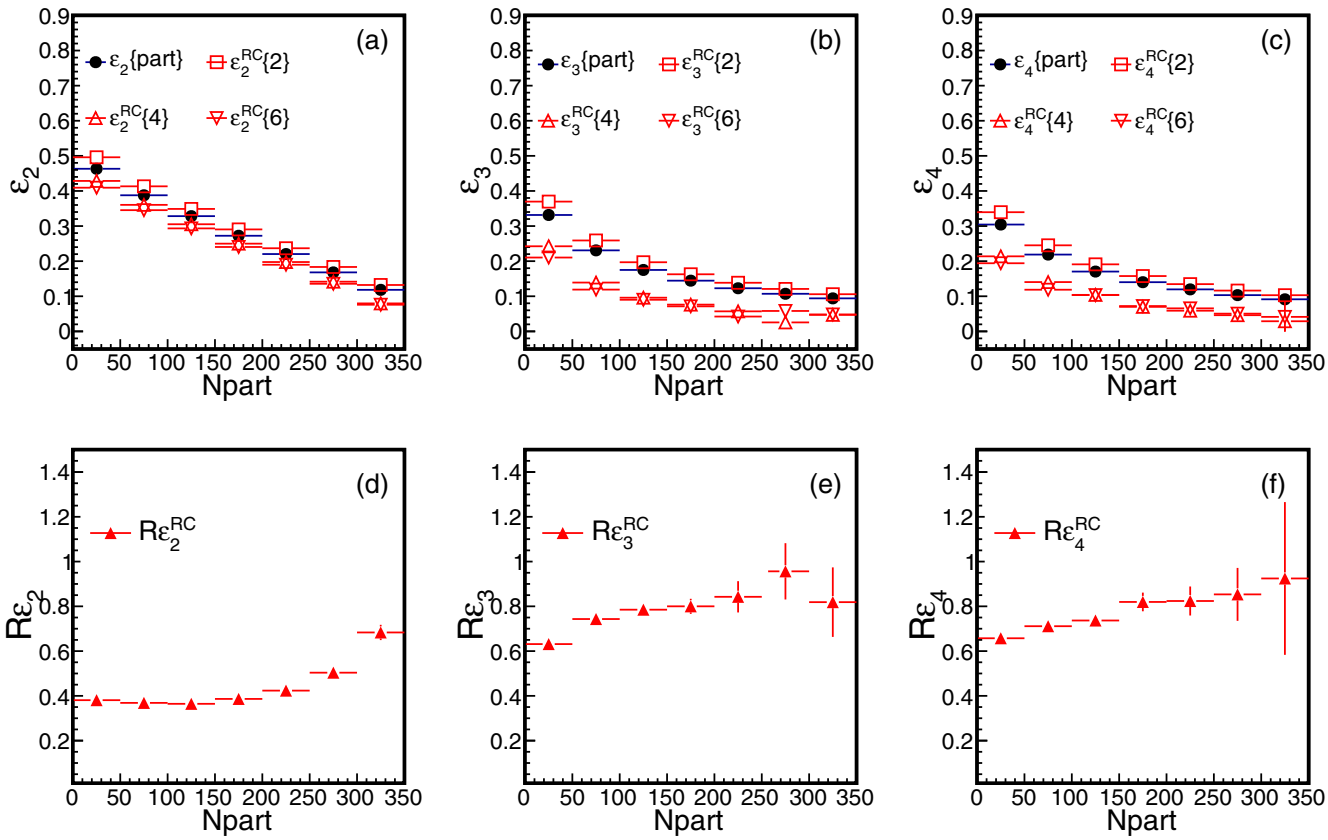

FIG. 1. Initial partonic eccentricity ε_n ($n = 2,3,4$) and their relative fluctuations defined by participant and regular cumulant methods as a function of mean number of participant nucleons $N_{\rm part}$. Eccentricities $\varepsilon_n\{2\}$, $\varepsilon_n\{4\}$, and $\varepsilon_n\{6\}$ defined based on Eq. (7) are denoted as $\varepsilon_n^{\rm RC}\{k\}$ ($k = 2,4,6$). Upper panels show initial partonic eccentricity ε_n in different orders of harmonics. Lower panels show relative fluctuations of eccentricities in different orders of harmonics defined by Eq. (14).

harmonics, fluctuations $R_{\varepsilon_n^{\rm RC}}$ $(n = 3,4)$ are larger than $R_{\varepsilon_2^{\rm RC}}$ for midcentral or peripheral collisions but comparable in magnitude for central collisions.

It has been shown that the relative magnitude of $v_n\{2\}$ and $v_n\{4\}$ depends on the fluctuations of v_n. Assuming that v_n is proportional to ε_n on an event-by-event basis, the following equation holds for higher orders $(n = 2,3,4)$:

$$\frac{v_n\{4\}}{v_n\{2\}} = \frac{\varepsilon_n\{4\}}{\varepsilon_n\{2\}} = \left(2 - \frac{\langle\varepsilon_n^4\rangle}{\langle\varepsilon_n^2\rangle^2}\right)^{-1}. \tag{15}$$

Fluctuations of v_n are supposed to stem from the fluctuations of ε_n [56]. Figure 2 displays ratios of cumulant eccentricities up to fourth order in the AMPT model using the regular cumulant method. $\varepsilon_n\{4\}/\varepsilon_n\{2\}$ shows a smooth decreasing trend from peripheral collisions to central collisions. The ratio is smaller than unity as expected due to the definition. The smaller is the eccentricity fluctuation, the closer the ratio is to unity. $v_n\{4\}/v_n\{2\}$ from AMPT and experimental flow measurements based on Q-cumulant which scale like the corresponding ratios of eccentricity cumulants are shown in comparison. It is found that $\varepsilon_2\{4\}/\varepsilon_2\{2\}$ are roughly equal to the ratio of the flow harmonic $v_2\{4\}/v_2\{2\}$ for nonperipheral collisions. Ratios of six-particle cumulant to four-particle cumulant $\varepsilon_2\{6\}/\varepsilon_2\{4\}$ is roughly equal to unity without seeing any centrality dependence, which is in consistent with the ratio of the flow harmonic $v_2\{6\}/v_2\{4\} \sim 1$. Ratio of higher-order harmonics $\varepsilon_n\{4\}/\varepsilon_n\{2\}$ and $\varepsilon_n\{6\}/\varepsilon_n\{4\}$ $(n = 3,4)$ are also shown providing additional constraints on the predictions of the ratio of the cumulant flow. Further experimental study of the ratio between cumulant flow harmonics may give access to the initial profile assuming the proportional relation between initial and final anisotropies [57,58].

Recent theoretical works show increasing interests in longitudinal features of the source created by relativistic heavy-ion collisions [59–62]. A model simulation shows that initial-state longitudinal fluctuations for second- and third-order harmonics survive the collective expansion resulting in a forward-backward asymmetry which propagate to the final stage during the source evolution [63]. Experimentally, flow measurements have been extended to study the longitudinal behavior of flow harmonics [64,65]. Due to the close relation between initial geometry and final flow harmonics, a systematic study of the longitudinal profile of the source is crucial for the understanding of the source evolution.

We perform here an investigation on the pseudorapidity η dependence of ε_n in the AMPT partonic stage of Au + Au collisions at 200 GeV. In the upper panels of Fig. 3, $\varepsilon_n\{\text{part}\}$ are shown as a function of pseudorapidity η for three different centrality classes, where two- and four-particle cumulants ε_n defined by Eq. (7) are plotted in addition to the participant $\varepsilon_n\{\text{part}\}$. Participant and cumulant eccentricity show almost

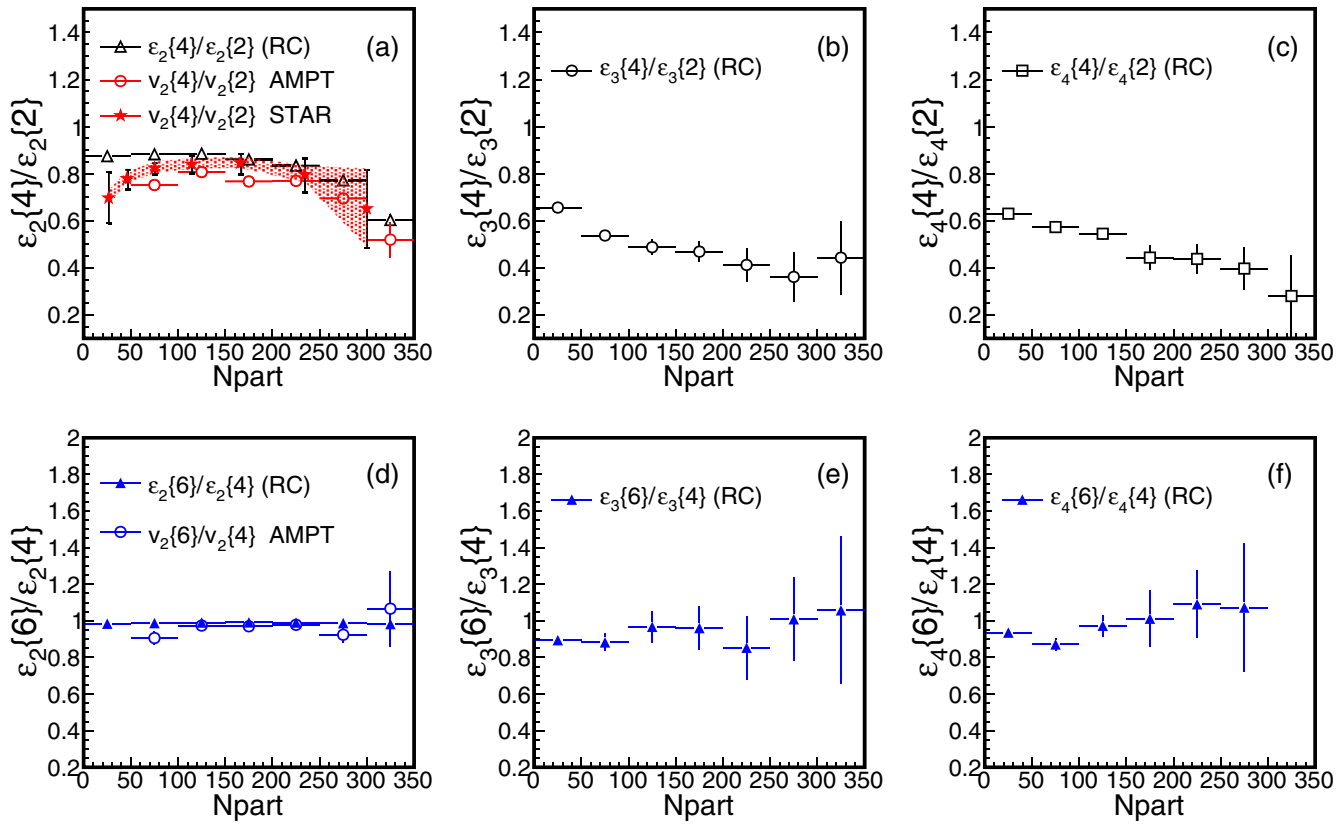

FIG. 2. Cumulant ratios $\varepsilon_n\{4\}/\varepsilon_n\{2\}$ and $\varepsilon_n\{6\}/\varepsilon_n\{4\}$ $(n = 2,3,4)$ as a function of $N_{\rm part}$. The eccentricities are defined with the regular cumulant method from Eq. (7) (denoted RC). Upper panels show cumulants ratio $\varepsilon_n\{4\}/\varepsilon_n\{2\}$ versus $N_{\rm part}$. Results of $v_n\{4\}/v_n\{2\}$ from both experiment measurement with Q-cumulant method and AMPT are also shown for comparison. Lower panels show cumulants ratio $\varepsilon_n\{6\}/\varepsilon_n\{4\}$ versus $N_{\rm part}$ from cumulant definitions.

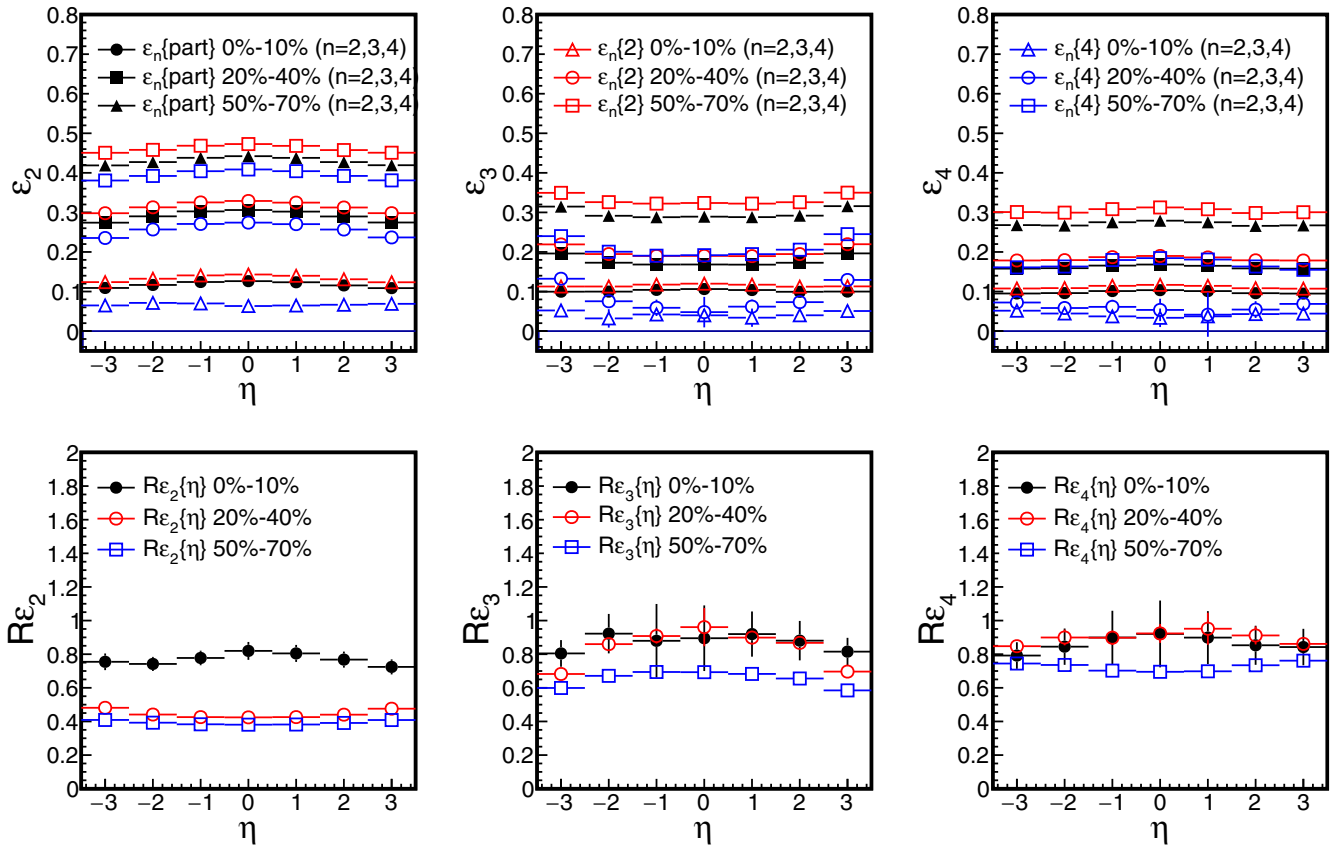

FIG. 3. Eccentricity coefficients ε_n ($n = 2,3,4$) defined with participant method and regular cumulant method as a function of pseudorapidity (η) for the AMPT initial condition. Fluctuations of ε_n are studied up to the fourth-order harmonic based on Eq. (14). Upper panel shows ε_n versus η defined by participant and cumulant method. Lower panel shows ε_n fluctuation up to the fourth order as a function of η. Results are shown for three selected centrality classes in Au + Au collisions at $\sqrt{s_{NN}} = 200$ GeV.

the same trend as a function of η. Comparing with the results of flow fluctuation in the AMPT calculations as shown in a previous study [23], $\varepsilon_2(\eta)$ is in a similar trend to $v_2(\eta)$ at the same centrality. $\varepsilon_3(\eta)$ or $\varepsilon_4(\eta)$ shows little η dependence which is quite different from corresponding flow harmonic $v_3(\eta)$ or $v_4(\eta)$. One possible cause might be from the partonic evolution process, but more investigations are needed for the final conclusion. As seen in the lower panel of Fig. 3, relative fluctuations of the participant eccentricity from regular cumulant definition R_{ε_n} ($n = 2,3,4$) show a symmetric profile as a function of pseudorapidity with a tiny η dependence for higher-order harmonics (n $\geqslant$ 3), which is quite similar to the flow fluctuation. As pseudorapidity dependencies of initial eccentricities reflect the longitudinal features of the created partonic matter, systematic comparison between eccentricity in model simulation and flow harmonic and their fluctuation properties in experiments are necessary to provide valuable information for a comprehensive understanding of the created source.

Besides investigating the pseudorapidity (η) dependence of eccentricity, it is also important to check the transverse-momentum (p_T) dependence of the initial eccentricity in a similar way as for flow harmonics, since flow harmonics stemming from the initial stage are expected to inherit mostly the p_T dependencies of the initial partonic anisotropies [66]. A recent study suggests that initial hard partons play an important role in the final harmonic flow formation [67]. A p_T tomographic study of the initial eccentricity is of great importance to check the anisotropy generation and afterburner development. In the AMPT model, initial partons decomposed from excited strings and minijet partons carry all the phase-space information, providing ideal conditions for study of source properties [68].

Figure 4 shows initial partonic eccentricities and their fluctuations as a function of transverse momentum p_T for three selected centrality classes. Similar p_T dependencies are for $n = 2$, 3, and 4, i.e., initial eccentricity increases as a function of parton transverse momentum. A general increasing trend can be observed for all the harmonics, suggesting that higher p_T partons contribute largely to the initial geometry anisotropy. The relative fluctuation of ε_n ($R_{\varepsilon_n}\{p_T\}$) from regular cumulant definitions are seen to be a smooth decreasing trend. R_{ε_2} at the low-p_T region is quite flat, which is quite similar to elliptic flow fluctuations. But a deviation trend from flow fluctuations can be observed at higher p_T. Higher-order ε_n (n $\geqslant$ 3) fluctuations show a monotonic decreasing trend at high p_T. Direct comparison between initial eccentricity fluctuation and final flow fluctuation as a function of p_T or η may not be straightforward because partonic multiscattering and final hadronic rescattering after hadron freeze-out might bring

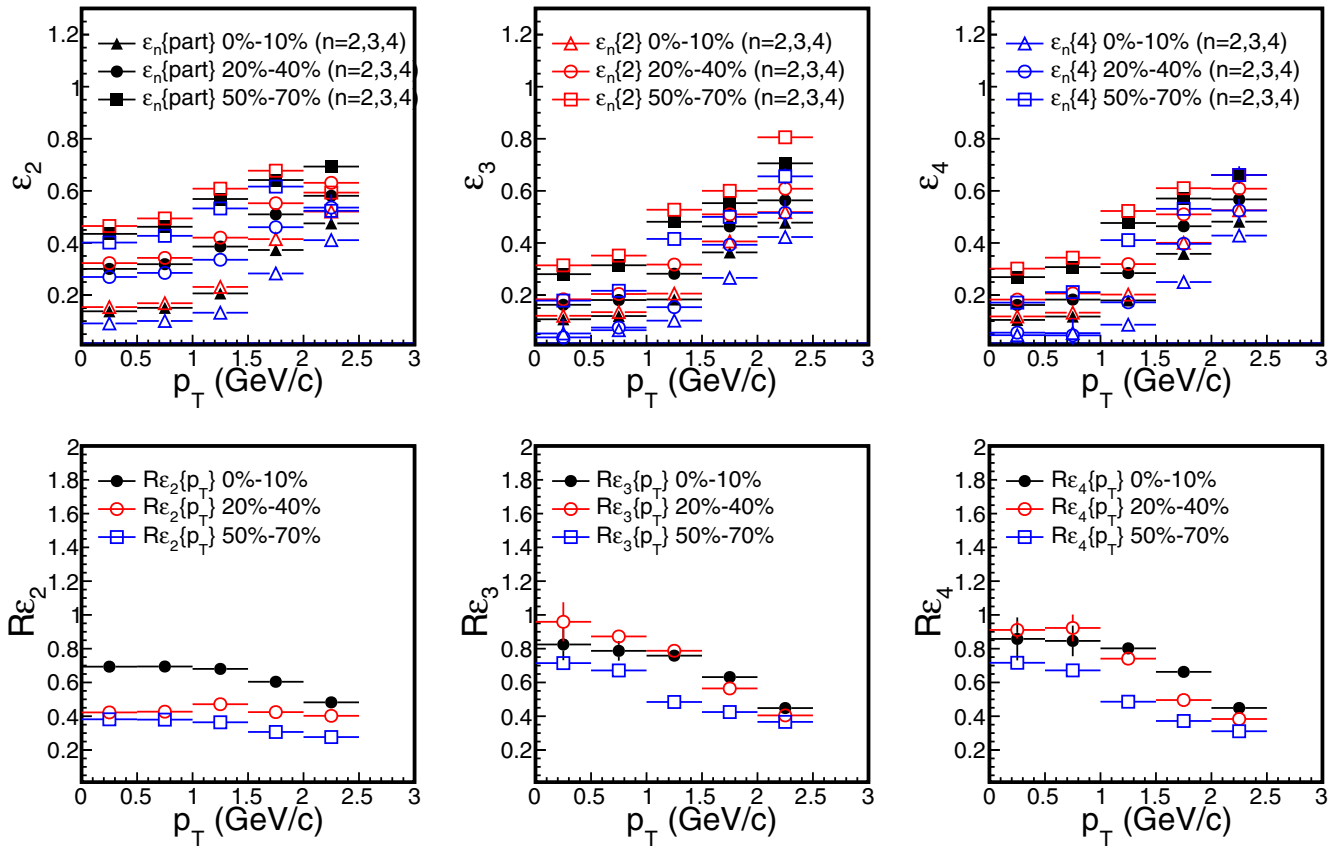

FIG. 4. Eccentricity coefficients ε_n ($n = 2,3,4$) defined with cumulant and participant method as a function of transverse momentum p_T for the AMPT initial condition. Upper panels show ε_n defined by participant and regular cumulants as a functions of p_T. Lower panels show ε_n ($n \geqslant 2$) fluctuations as a functions of p_T, where ε_n fluctuation is defined by Eq. (14). Results are shown for three different centrality classes in Au + Au collisions at $\sqrt{s_{NN}} = 200$ GeV.

in some substantial effects on the anisotropy development. Nevertheless, our results suggest that initial ε_n fluctuation as a function of transverse momentum p_T or pseudorapidity η provides additional information of the source evolution. Further study not only on the pseudorapidity or transverse momentum dependence of ε_n but also on correlations between quantities at different transverse momentum or rapidity bins with AMPT model simulation will provide a comprehensive understanding for the source anisotropy as motivated by studies [60,69].

B. Harmonic flow response to initial eccentricity in multiphase transport model

In ideal hydrodynamics, a linear correlation is predicted between initial source geometric anisotropy and final flow of hadrons. In the past few years, impressive progress has been made in studying flow response to the initial stage [7,48,70]. We understand that elliptic flow v_2 and triangular flow v_3 are driven mainly by the linear response to the initially produced fireball. For higher-order harmonics, due to nonlinear responses, the conversion of the initial geometry to the final flow becomes much more complicated which need to consider combinatorial contributions from different orders of eccentricity harmonics, as suggested by a realistic simulation study [71]. Taking the ratio v_n/ε_n as the conversion coefficient from the initial eccentricity to the final flow, we further studied the ratio $v_n\{k\}/\varepsilon_n\{k\}$ ($k = 4,6$) with the cumulant method and compared with results from the participant method. In Fig. 5, we plot the conversion coefficient v_n/ε_n ($n = 2,3$) as a function of number of participant nucleons, $N_{\rm part}$. $v_n\{k\}/\varepsilon_n\{k\}$ (k $\geqslant$ 2) are based on cumulant definition Eq. (7). Experimental measurements of $v_2\{2\}/\varepsilon_2\{2\}$ and $v_2\{4\}/\varepsilon_2\{4\}$ with elliptic flow v_2 measured with the Q-cumulant method where ε_2 with the regular cumulant method based on the MC-Glauber model is shown for comparison.

In a similar way as in experimental measurements, when $v_2\{k\}$ ($k = 2,4$) scaled with cumulant $\varepsilon_2\{k\}$ ($k = 2,4$), AMPT reproduces well the experimental results. The conversion coefficient from participant definition $v_2\{\text{part}\}/\varepsilon_2\{\text{part}\}$ follows a similar trend as the cumulant $v_2\{k\}/\varepsilon_2\{k\}$ ($k = 2,4,6$). The trend of v_n/ε_n shows the hierarchy that $v_2\{2\}/\varepsilon_2\{2\}$ is systematically higher than higher-order cumulant $v_2\{k\}/\varepsilon_2\{k\}$ ($k = 4,6$) over the whole centrality region. Further specific study of the conversion coefficient of the initial profile considering linear and nonlinear hydrodynamic responses is expected to provide more qualitative descriptions [71,72].

Recent studies suggest that hard probes like jets are prospective for tomographic studies of the initial source profile and harmonic fluctuations in the initial states

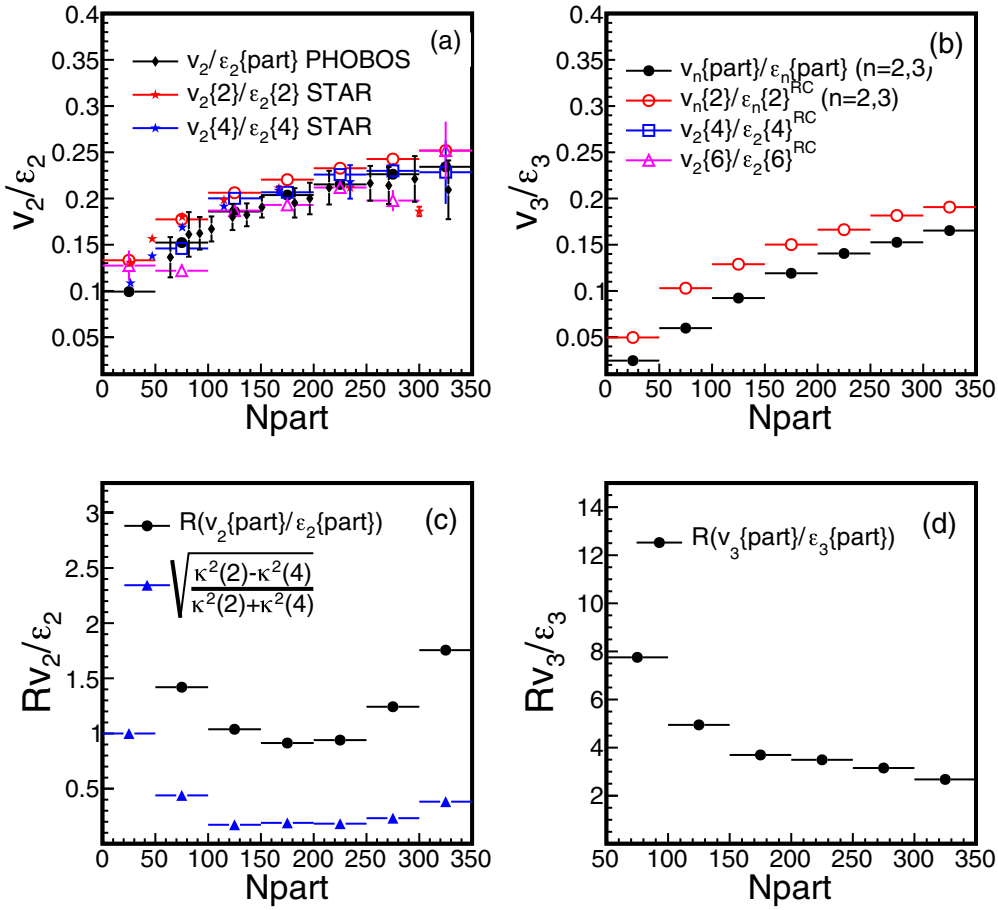

FIG. 5. Conversion coefficient v_n/ε_n ($n = 2,3$) and their fluctuation as a function of N_{part}. $v_n\{\text{part}\}/\varepsilon_n\{\text{part}\}$ from participant method and $v_n\{k\}/\varepsilon_n\{k\}$ ($k = 2,4,6$) from the cumulant method [Eq. (7)]. (a), (b) v_n/ε_n versus N_{part} for different harmonic orders. The experimental results of $v_n\{2\}/\varepsilon_n\{2\}$ and $v_n\{4\}/\varepsilon_n\{4\}$ with flow measured in Q-cumulant method and eccentricity in regular cumulant method are shown for comparison. (c), (d) Fluctuation of conversion coefficient v_n/ε_n ($n = 2,3$) as a function of N_{part}, where $\kappa(2) = v_2\{2\}/\varepsilon_2\{2\}$ and $\kappa(4) = v_2\{4\}/\varepsilon_2\{4\}$.

[73–75]. Motivated by this idea, we study the final hadron flow responses to the initial parton eccentricity as a function of transverse momentum p_T. Figure 6 shows the p_T dependence of the coefficient v_n/ε_n from both the cumulant method and the participant method. We can see that $v_n(p_T)/\varepsilon_n$ generally shows an increasing trend as a function of p_T. For both

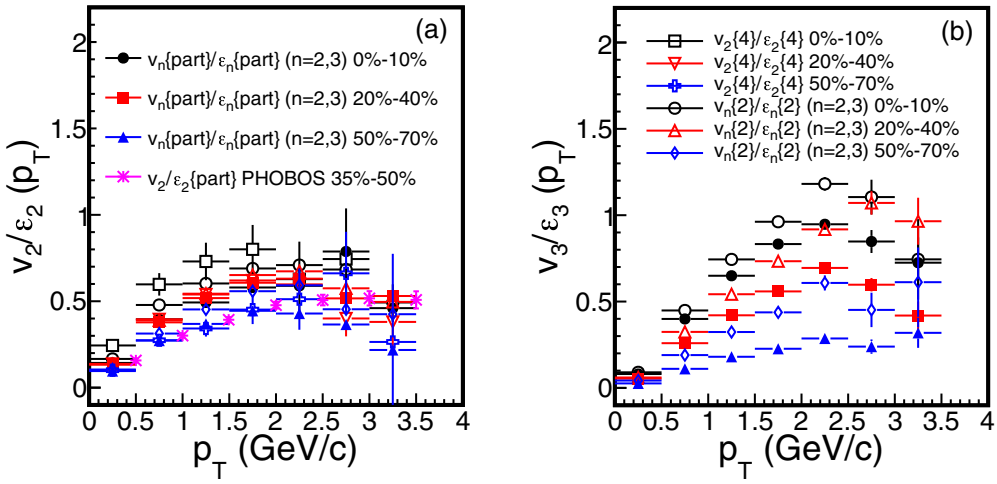

FIG. 6. Conversion coefficients v_n/ε_n ($n = 2,3$) as a function of transverse momentum p_T. v_n/ε_n from the participant method and the regular cumulant method are studied.

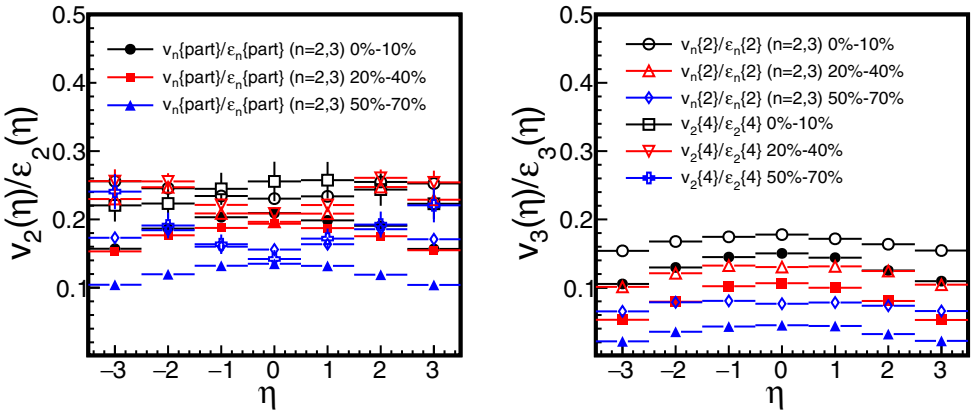

FIG. 7. Conversion coefficients v_n/ε_n ($n = 2,3$) as a function of pseudorapidity η. v_n/ε_n from the traditional participant method and the regular cumulant method (RC) are studied.

cumulant and participant v_n/ε_n, one can see that the conversion efficiency tends to be larger at higher p_T. The centrality dependence of $v_n(p_T)/\varepsilon_n$ is presented by investigating three centrality classes from central to peripheral collisions. More simulation data are needed to extend to an even-higher-p_T region to study the hard jet response. In additional to the study of p_T dependence, the pseudorapidity η dependence of v_n/ε_n ($n = 2,3$) are also studied by looking into the ratio of $v_n(\eta)$ to $\varepsilon_n(\eta)$ at the corresponding rapidity region. The flow response to the initial eccentricity in the longitudinal direction is studied. Results of $v_n(\eta)/\varepsilon_n(\eta)$ are shown in Fig. 7 with a symmetric shape observed. Both $v_n(\eta)/\varepsilon_n(\eta)$ ($n = 2,3$) from both the participant definition and the regular cumulant definition are found to be quite similar to the distribution of corresponding $v_n(\eta)$ which shows a slight η dependence. Cumulants $v_n(\eta)/\varepsilon_n(\eta)$ ($n = 2,3$) show weaker η dependence in comparison with participants $v_n(\eta)/\varepsilon_n(\eta)$ ($n = 2,3$), which suggests the proportionality between ε_n at fixed spatial rapidity and v_n at fixed pseudorapidity changes little in the longitudinal direction.

C. Partonic effect on eccentricity and eccentricity fluctuation

The parton scattering cross section in the AMPT model has shown considerable influence on the magnitude of the flow coefficients [15]. It is important to investigate the effect on eccentricity and eccentricity fluctuation in the partonic stage since it may shed light on the evolution of the source in heavy-ion collision. Figure 8 (upper panel) shows the source participant eccentricity before (denoted as "initial") and after (denoted as "final") partonic scatterings for different orders of harmonics as a function of mean value of participant nucleons for partons in Au + Au collisions from the AMPT simulations. Parton scattering cross sections were selected as 3 and 10 mb. It indicates that partonic scattering significantly reduces eccentricity commonly for all orders of harmonics. We find for noncentral collisions the larger partonic cross section, the smaller final ε_n after partonic scattering but for central collisions the partonic scattering cross section has little effect on the source eccentricity ε_n.

The relative fluctuation of participant $\varepsilon_n\{\text{part}\} - R_{\varepsilon_n^{\text{part}}}$ ($n \geqslant 2$) are shown in the lower panels of Fig. 8, where we give the comparison of fluctuation $R_{\varepsilon_n^{\text{part}}}$ before and after partonic scatterings with two different partonic cross sections. Partonic scattering dramatically increases the fluctuation of $\varepsilon_n\{\text{part}\}$ for different orders of harmonics. Experimental measurements of higher-order flow fluctuations with the cumulant method will be prospective for quantitatively understanding the development of anisotropy fluctuation from the initial partonic stage to the final hadronic stage.

IV. SUMMARY

In summary, within the framework of a multiphase transport model (AMPT), initial partonic eccentricity and eccentricity fluctuations are studied up to fourth order of harmonic by means of the traditional participant method and multiparticle cumulant method in Au + Au collisions at a center-of-mass energy of 200 GeV. Eccentricities ε_n and fluctuations R_{ε_n} defined by the participant method and the regular cumulant method are studied and compared systematically. Eccentricity fluctuation shows a similar picture as flow fluctuation, which confirms the close relationship between initial eccentricity harmonics and final flow harmonics. Flow responses are investigated by the ratio v_n/ε_n as a function of number of participant nucleons (N_{part}), transverse momentum (p_T), and pseudorapidity (η) for a tomographic study of the conversion properties. Relative fluctuations of ε_n defined by cumulants as a function of transverse momentum and pseudorapidity are also studied specifically for the transverse and longitudinal features of the created source. ε_n fluctuation versus p_T and η show similar trends as the corresponding flow harmonic and flow fluctuation measured experimentally. Higher harmonic eccentricity fluctuation studies are expected to give further constraint to higher-order harmonic flow studies.

Similar to anisotropic flow measurements which have been proved to be sensitive to the shape and shape fluctuation of the initial overlap zone, direct measurements of eccentricity fluctuations could lead to a better understanding of the initial source conditions. Through the comparison of the AMPT model

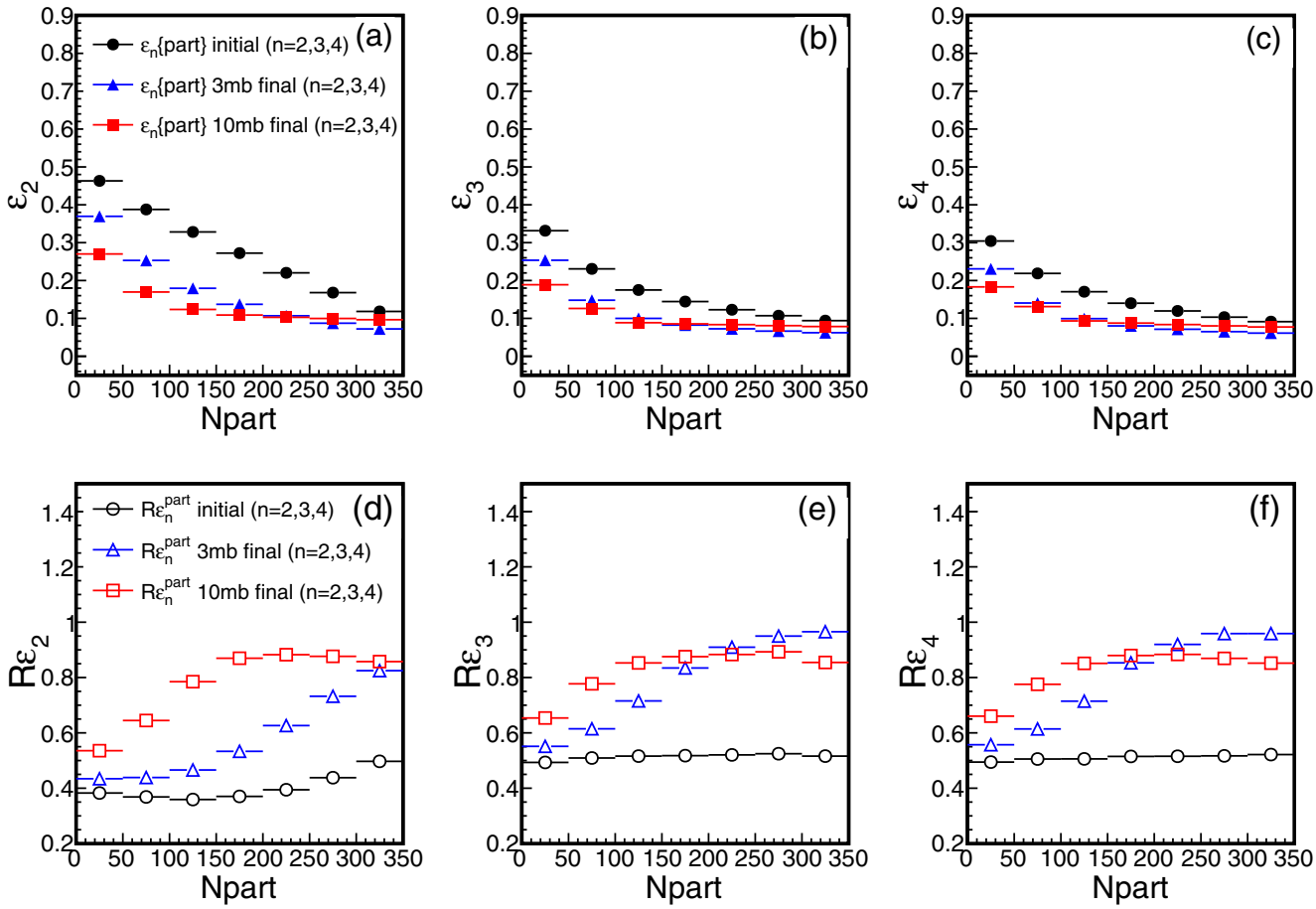

FIG. 8. Eccentricity and fluctuation as a function of mean value of participant nucleons $N_{\rm part}$ in AMPT model for Au + Au collision at 200 GeV. Upper panels show ε_n {part} before (denoted as "initial") and after (denoted as "final") partonic scatterings with two parton cross-section settings of 3 and 10 mb. Lower panels show ε_n {part} fluctuation $R_{\varepsilon_n^{\rm part}}$ before and after partonic scatterings.

simulation results with experimental measurements, we found that ellipticity and triangularity as well as higher harmonic initial anisotropies show similar behavior as final flow harmonics both in the transverse and longitudinal directions. As event-by-event fluctuations are crucial to the current understanding of relativistic heavy-ion collisions, the study of the physics origin of how fluctuations of flow harmonics stem from the early stage of collision will be of great importance. The AMPT model simulations provide a promising way of studying the initial partonic state. Future experimental study of anisotropic flow harmonics with extended p_T region and η region can provide further constraints on the initial source profile. We also expect studies on the initial fluctuations in smaller systems, such as p + Au, d + Au, or ^{3}He +Au, especially the fluctuation properties in the longitudinal direction can bring complementary information of the source evolution mechanisms.

ACKNOWLEDGMENTS

This work is supported by the Major State Basic Research Development Program in China under Grant No. 2014CB845400, the National Natural Science Foundation of China under Grants No. 11421505, No. 11220101005, No.11522547. and No. 11375251, and the Youth Innovation Promotion Association of CAS under Grant No. 2013175.

[1] J.-Y. Ollitrault, Phys. Rev. D **46**, 229 (1992).
[2] S. A. Voloshin, A. M. Poskanzer, and R. Snellings, arXiv:0809.2949.
[3] P. F. Kolb, J. Sollfrank, and U. W. Heinz, Phys. Lett. B **459**, 667 (1999).
[4] K. H. Ackermann *et al.* (STAR Collaboration), Phys. Rev. Lett. **86**, 402 (2001).
[5] D. Teaney, J. Lauret, and E. V. Shuryak, Phys. Rev. Lett. **86**, 4783 (2001).
[6] P. Romatschke and U. Romatschke, Phys. Rev. Lett. **99**, 172301 (2007).
[7] H. Song, S. A. Bass, U. Heinz, T. Hirano, and C. Shen, Phys. Rev. Lett. **106**, 192301 (2011).
[8] C. M. Ko *et al.*, Nucl. Sci. Tech. **24**, 050525 (2013).

[9] U. Heinz, J. Phys. G **31**, S717 (2005).
[10] C. Gale, S. Jeon, and B. Schenke, Int. J. Mod. Phys. A **28**, 1340011 (2013).
[11] Z. Qiu and U. Heinz, AIP Conf. Proc. **1441**, 774 (2012).
[12] J. Adams *et al.* (STAR Collaboration), Phys. Rev. Lett. **92**, 062301 (2004).
[13] L. Adamczyk *et al.* (STAR Collaboration), Phys. Rev. C **88**, 014904 (2013).
[14] A. Adare *et al.* (PHENIX Collaboration), Phys. Rev. Lett. **107**, 252301 (2011).
[15] L.-W. Chen, C. M. Ko, and Z.-W. Lin, Phys. Rev. C **69**, 031901 (2004).
[16] L. X. Han, G. L. Ma, Y. G. Ma, X. Z. Cai, J. H. Chen, S. Zhang, and C. Zhong, Phys. Rev. C **84**, 064907 (2011).
[17] A. Adare *et al.* (PHENIX Collaboration), Phys. Rev. C **93**, 051902(R) (2016).
[18] B. Alver and G. Roland, Phys. Rev. C **81**, 054905 (2010).
[19] B. Schenke, S. Jeon, and C. Gale, Phys. Rev. Lett. **106**, 042301 (2011).
[20] B. Schenke, S. Jeon, and C. Gale, Phys. Rev. C **85**, 024901 (2012).
[21] R. Andrade, F. Grassi, Y. Hama, T. Kodama, and O. Socolowski, Phys. Rev. Lett. **97**, 202302 (2006).
[22] H. Petersen, G.-Y. Qin, S. A. Bass, and B. Müller, Phys. Rev. C **82**, 041901 (2010).
[23] L. Ma, G. L. Ma, and Y. G. Ma, Phys. Rev. C **89**, 044907 (2014).
[24] P. Sorensen, J. Phys. G **34**, S897 (2007).
[25] B. Alver *et al.* (PHOBOS Collaboratin), J. Phys. G **34**, S907 (2007).
[26] B. Alver, B. B. Back *et al.*, Phys. Rev. Lett. **104**, 142301 (2010).
[27] G. Agakishiev *et al.* (STAR Collaboration), Phys. Rev. C **86**, 014904 (2012).
[28] H. Holopainen, H. Niemi, and K. J. Eskola, Phys. Rev. C **83**, 034901 (2011).
[29] B. H. Alver, C. Gombeaud, M. Luzum, and J.-Y. Ollitrault, Phys. Rev. C **82**, 034913 (2010).
[30] M. Miller and R. Snellings, arXiv:nucl-ex/0312008.
[31] R. D. de Souza, J. Takahashi, T. Kodama, and P. Sorensen, Phys. Rev. C **85**, 054909 (2012).
[32] G.-L. Ma and X.-N. Wang, Phys. Rev. Lett. **106**, 162301 (2011).
[33] J. Wang, Y. Ma, G. Zhang, D. Fang, L. Han, and W. Shen, Nucl. Sci. Tech. **24**, 030501 (2013).
[34] J. Wang, Y. G. Ma, G. Q. Zhang, and W. Q. Shen, Phys. Rev. C **90**, 054601 (2014).
[35] B. Alver, B. B. Back *et al.*, Phys. Rev. Lett. **98**, 242302 (2007).
[36] H.-J. Drescher and Y. Nara, Phys. Rev. C **76**, 041903 (2007).
[37] W. Broniowski, P. Bożek, and M. Rybczyński, Phys. Rev. C **76**, 054905 (2007).
[38] B. Zhang, C. M. Ko, B.-A. Li, and Z. Lin, Phys. Rev. C **61**, 067901 (2000).
[39] X.-N. Wang and M. Gyulassy, Phys. Rev. D **44**, 3501 (1991).
[40] B. Zhang, Comput. Phys. Commun. **109**, 193 (1998).
[41] Z.-W. Lin, C. M. Ko, B.-A. Li, B. Zhang, and S. Pal, Phys. Rev. C **72**, 064901 (2005).
[42] J. Xu and C. M. Ko, Phys. Rev. C **84**, 014903 (2011).
[43] Y. J. Ye, J. H. Chen, Y. G. Ma, S. Zhang, and C. Zhong, Phys. Rev. C **93**, 044904 (2016).
[44] Y.-F. Xu, Y.-J. Ye, J.-H. Chen, Y.-G. Ma, S. Zhang, and C. Zhong, Nucl. Sci. Tech. **27**, 87 (2016).
[45] Z.-w. Lin, S. Pal, C. M. Ko, B.-A. Li, and B. Zhang, Phys. Rev. C **64**, 011902(R) (2001).
[46] S. A. Voloshin, A. M. Poskanzer, A. Tang, and G. Wang, Phys. Lett. B **659**, 537 (2008).
[47] Z. Qiu and U. W. Heinz, Phys. Rev. C **84**, 024911 (2011).
[48] H. Petersen, R. La Placa, and S. A. Bass, J. Phys. G **39**, 055102 (2012).
[49] S. A. Voloshin, arXiv:nucl-th/0606022.
[50] R. S. Bhalerao and J.-Y. Ollitrault, Phys. Lett. B **641**, 260 (2006).
[51] A. Bilandzic, R. Snellings, and S. Voloshin, Phys. Rev. C **83**, 044913 (2011).
[52] Y. Zhou, K. Xiao, Z. Feng, F. Liu, and R. Snellings, Phys. Rev. C **93**, 034909 (2016).
[53] B. B. Abelev *et al.* (ALICE Collaboration), Phys. Rev. C **90**, 054901 (2014).
[54] C. Adler, Z. Ahammed *et al.*, Phys. Rev. C **66**, 034904 (2002).
[55] R. A. Lacey, R. Wei, J. Jai, N. N. Ajitanand, J. M. Alexander, and A. Taranenko, Phys. Rev. C **83**, 044902 (2011).
[56] R. S. Bhalerao, M. Luzum, and J.-Y. Ollitrault, Phys. Rev. C **84**, 054901 (2011).
[57] L. Yan and J.-Y. Ollitrault, Phys. Rev. Lett. **112**, 082301 (2014).
[58] L. Yan, J.-Y. Ollitrault, and A. M. Poskanzer, Phys. Rev. C **90**, 024903 (2014).
[59] L. Pang, Q. Wang, and X.-N. Wang, Phys. Rev. C **86**, 024911 (2012).
[60] L.-G. Pang, H. Petersen, G.-Y. Qin, V. Roy, and X.-N. Wang, Eur. Phys. J. A **52**, 97 (2016).
[61] P. Bozek, A. Bzdak, and G.-L. Ma, Phys. Lett. B **748**, 301 (2015).
[62] K. Xiao, F. Liu, and F. Wang, Phys. Rev. C **87**, 011901 (2013).
[63] J. Jia and P. Huo, Phys. Rev. C **90**, 034915 (2014).
[64] B. B. Back *et al.* (PHOBOS Collaboration), Phys. Rev. C **72**, 051901 (2005).
[65] J. Adam *et al.* (ALICE Collaboration), Phys. Lett. B (2016).
[66] P. F. Kolb, L.-W. Chen, V. Greco, and C. M. Ko, Phys. Rev. C **69**, 051901 (2004).
[67] M. Schulc and B. Tomasik, Phys. Rev. C **90**, 064910 (2014).
[68] M. Nie and G. Ma, Nucl. Tech. (in Chinese) **37**, 100519 (2014).
[69] Khachatryan *et al.* (CMS Collaboration), Phys. Rev. C **92**, 034911 (2015).
[70] R. A. Lacey, A. Taranenko, J. Jia, D. Reynolds, N. N. Ajitanand, J. M. Alexander, Y. Gu, and A. Mwai, Phys. Rev. Lett. **112**, 082302 (2014).
[71] F. G. Gardim, F. Grassi, M. Luzum, and J.-Y. Ollitrault, Phys. Rev. C **85**, 024908 (2012).
[72] J. Jia, J. Phys. G **41**, 124003 (2014).
[73] X. Zhang and J. Liao, Phys. Rev. C **89**, 014907 (2014).
[74] X.-L. Zhang and J.-F. Liao, Phys. Lett. B **713**, 35 (2012).
[75] M. W. Nie and G. L. Ma, Phys. Rev. C **90**, 014907 (2014).